

# Highly *N,P*-doped carbon dots: Rational design, photoluminescence and cellular imaging

Junjian Li<sup>1</sup> · Yingzhi Jiao<sup>2</sup> · Liandong Feng<sup>3</sup> · Ying Zhong<sup>1</sup> · Gancheng Zuo<sup>1</sup> · Aming Xie<sup>1</sup> · Wei Dong<sup>1</sup>

Received: 14 February 2017 / Accepted: 26 April 2017 / Published online: 10 May 2017  
© Springer-Verlag Wien 2017

**Abstract** The authors describe the synthesis of carbon dots (CDs) that are highly doped with both nitrogen and phosphorus. Synthesis is accomplished via a hydrothermal reaction starting from diethylenetriaminepenta(methylenephosphonic acid) and *m*-phenylenediamine as the precursors. The high *N,P*-doping ratios renders the codoped CDs excellently water soluble, photostable over a wide range of pH values, and photostable in the presence of various metal ions. Ferric ions acts as a strong quencher of fluorescence. Their low cytotoxicity and strong green fluorescence (with excitation/emission peaks at 440/510 nm and a quantum yield of 0.32) make the CDs well suited for purposes of cell imaging, and this is demonstrated by fluorescent bioimaging of human lung carcinoma cells (type A549) and human breast cancer cells (type KB). Furthermore, the CDs were used as an effective probe for monitoring Fe(III) in both aqueous solution and living cells.

**Keywords** Hydrothermal synthesis · Metal ion sensor · Living cells · Zeta potential · Nanomaterials

## Introduction

Semiconductor quantum dots (SQDs) possess high brightness and photo-stability and have been deemed as one of the most promising alternatives instead of traditional organic fluorophores. But they are limited in various areas of applications especially in bio-imaging of living cells, on account of their composing of toxic elements including cadmium (Cd), lead (Pb), and mercury (Hg) [1, 2]. To avoid this drawback, carbon dots (CDs) emerge and progress rapidly in a broad fields of applications such as sensing, [3–5] bioimaging, [6–9] nanomedicine, [10] photocatalysis, [11–14] and optoelectronics, [10] due to their not only good biocompatibility but also excellent photostability, highly tunable photoluminescence (PL) property, chemical inertness and high photo-conversion. However, there are still shortcomings for most reported CDs in many applications, particularly in the biology-relevant fields. Firstly, the emission spectrum of most CDs mainly focused on the blue-light region rather than the long-wavelength region (i.e., green- to red-light). [15] Secondly, the lack of strong hydrophilic groups such as sulfonate, phosphate or polyhydroxyl moieties, led to poor solubility or photo-stability in relatively acidic or alkalic aqueous solution, resulting in narrowed application scopes of CDs. [3, 4, 6] Thirdly, the weak resistance to metal ion interference may cause adverse effect on highly efficient bio-imaging [16]. Therefore, the design of CDs that emitting at long-wavelength along with high aqueous

**Electronic supplementary material** The online version of this article (doi:10.1007/s00604-017-2314-0) contains supplementary material, which is available to authorized users.

✉ Liandong Feng  
fengliand@126.com

✉ Wei Dong  
weidong@njust.edu.cn

<sup>1</sup> School of Chemical Engineering, Nanjing University of Science & Technology, Nanjing 210094, China

<sup>2</sup> Department of Scientific Research, Nanjing Huawei Medicine Technology Development co., LTD, Nanjing 210023, China

<sup>3</sup> State Key Laboratory of Analytical Chemistry for Life Science, School of Chemistry and Chemical Engineering, Nanjing University, Nanjing 210093, China

solubility, photo-stability and high interference resistance is strongly desirable, but this target has been rarely achieved up to now [17].

Generally, CDs were designed and synthesized via the “top-down” or “bottom-up” approach. Comparing to the “top-down” approach involving the breaking down of larger carbon structures, [18–20] the “bottom-up” way referred the preparation of CDs from a wide range of small molecular precursors including citrate, [21, 22] carbohydrates [23, 24] or their combinations by solvothermal treatments, and microwave-assisted synthesis, and thus furnished easier synthetic processes and more flexible adjustability of chemical surface structure, photoluminescence, aqueous solubility as well as pH photo-stability. To prolong emission wavelengths and improve quantum yields (QYs) of CDs, heteroatom doping was frequently used, especially *N*-doping. For example, N source in aminobenzene or formamide can intensely prolong the emissive wavelength of the as-prepared CDs by a simple solvothermal process, in spite of low-stable decentrality in water and weak resistance to metal ion interference, acid or base. [6, 25].

To avoid these drawbacks, P element was frequently employed to dope the *N*-doped CDs to form *N,P*-codoped CDs, which can distinctly improve the water decentrality. Recently, there were a few researches focusing on the *N,P*-codoped CDs, where aliphatic amine/ $\text{NH}_3\text{-H}_2\text{O}$ , phosphoric acid were employed as the N, P sources, respectively. [15–17] In these research, the doping ratios of N, P were relative low and emissive wavelength preferred to the blue region. Furthermore, these *N,P*-codoped CDs are sensitive to  $\text{Fe}^{3+}$  even under low concentration. [16] If using organic phosphoric acid with several phosphate groups and N atom as both N and P dopants as well as employing aromatic amine as additional N source and conjugative monomer instead of aliphatic amines or  $\text{NH}_3\text{-H}_2\text{O}$ , *N,P*-codoping ratio should be distinctly enlarged, and thus this may result in the various variations of CDs on emission wavelengths, decentrality, resistance to metal ion interference, and pH sensibility. Herein, we have designed and synthesized a novel *N,P*-codoped carbon dots (DAP-CDs) using diethylenetriaminepenta (methylenephosphonic acid) (DAP) and *m*-phenylenediamine as the precursors through a simple hydrothermal process. The as-prepared CDs has a higher *N,P*-codoping ratios and displayed significantly enhanced dispersibility and photo-stability in a broad range of pH values. Under the stimulation of ultraviolet or blue light, these CDs only emitted single but intense green fluorescence and kept photo-stability when contacted with various metal ions. High biocompatibility was observed from the MTT test and high-quality cell imaging images can be obtained, indicating huge potential in the field of bio-imaging.

## Material and methods

### Reagents and materials

*m*-Phenylenediamine and 70 wt.% of aqueous DAP were purchased from Adamas Scientific Co., Ltd. (Shanghai, China, <http://www.adamas-beta.com/home!home.action>) and used without purification.  $\text{AgNO}_3$ ,  $\text{CoCl}_2\cdot 6\text{H}_2\text{O}$ ,  $\text{Pb}(\text{NO}_3)_2$ ,  $\text{CdCl}_2$ ,  $\text{CrCl}_3\cdot 6\text{H}_2\text{O}$ ,  $\text{MgCl}_2\cdot 6\text{H}_2\text{O}$ ,  $\text{CuCl}_2\cdot 2\text{H}_2\text{O}$ ,  $\text{ZnCl}_2$ ,  $\text{CaCl}_2$ ,  $\text{KCl}$ ,  $\text{NaCl}$ ,  $\text{NiCl}_2\cdot 6\text{H}_2\text{O}$ ,  $\text{HgCl}_2$  and  $\text{FeCl}_3\cdot 6\text{H}_2\text{O}$  were purchased from Energy Chemical (Shanghai, China, <http://www.energy-chemical.com.cn/>). Dialysis membrane (1000 MWCO, Shanghai Canspec Scientific Instruments Co., Ltd. China, <http://www.canspecsci.com/>) was washed with deionized water before use. Deionized water was obtained from Direct-Q3 UV, Millipore. *m*-Phenylenediamine was chose to introduction of conjugated structure. The DAP was used here because of its high N and  $\text{PO}_3\text{H}_2$  contents.

### Characterization

DAP-CDs was observed on a high resolution transmission electron microscope (HRTEM, Tecnai G2 F20, FEI). X-ray photoelectron spectra (XPS) was carried out in a Thermo Scientific ESCALAB 250Xi X-ray photoelectron spectrometer equipped with a monochromatic Al K $\alpha$  X-ray source (1486.6 eV). The crystal patterns were measured on X-ray diffractometer (XRD, X'Pert Pro, Philips), using Cu K ( $\lambda = 1.54 \text{ \AA}$ ) radiation. Fourier transform infrared (FTIR) spectra were recorded on a Nicolet iS10 FTIR instrument (Thermo Fisher Scientific, USA).

### Synthesis of the DAP-CDs

Firstly, 0.5 g of *m*-phenylenediamine and 2.84 g of DAP (aqueous 70 wt.%) were dissolved in 30 mL of deionized water, and the solution was then transferred into a Teflon autoclave. After heating at 200 °C for 5 h, the autoclave was cooled down to room temperature, naturally. After that, the obtained DAP-CDs solution was subsequently centrifuged at 10000 rpm to remove impurities with high molecular weights and the residual liquid was dialyzed in a dialysis membrane (1000 MWCO, Shanghai Green Bird Science & Technology Development Co., China) for 2 days to remove other small molecules. Finally, the DAP-CDs were collected by a freeze drying process.

### Fluorescence assay

All spectrum experiments were performed in solution [0.01 M HEPES buffer, pH 7.4] on fluorescence spectrometer experiments. In the fluorescence spectra of the DAP-CDs ( $5 \mu\text{g}\cdot\text{mL}^{-1}$ ) were recorded upon the addition of  $4 \text{ mmol}\cdot\text{L}^{-1}$  of other salts ( $\text{Fe}^{3+}$ ,  $\text{Ag}^+$ ,  $\text{Pb}^{2+}$ ,  $\text{Cd}^{2+}$ ,  $\text{Cr}^{3+}$ ,  $\text{Mg}^{2+}$ ,  $\text{Cu}^{2+}$ ,  $\text{Zn}^{2+}$ ,  $\text{Ca}^{2+}$ ,  $\text{Ni}^{2+}$ ,  $\text{Hg}^{2+}$  and  $\text{Co}^{3+}$ ). In fluorescence spectra titration

experiments, DAP-CDs ( $5 \mu\text{g}\cdot\text{mL}^{-1}$ ) dispersion was added into HEPES, followed by the addition of  $\text{Fe}^{3+}$  standard with various concentrations.

### Fluorescence quantum yield QY measurements

The relative fluorescence QY ( $\Phi$ ) of the DAP-CDs was calculated using the equation:

$$\Phi = \Phi_{\text{R}} \frac{I}{I_{\text{R}}} \frac{A_{\text{R}}}{A} \frac{n^2}{n_{\text{R}}^2}$$

The optical densities were measured using a Shimadzu UV-2550 spectrometer and Shimadzu RF-5301 fluorescence spectro-photometer. Where  $\Phi$  is fluorescence quantum yield,  $I$  is the integrated fluorescence intensity,  $n$  is the refractive index of solvent, and  $A$  is the optical density (absorption). The subscript R refers to the reference of Fluorescein.

### Cytotoxicity investigation and fluorescence imaging of living cells

Human lung carcinoma cells (type A549) and human breast cancer cells (type KB cells) ( $1 \times 10^4$  cells/well) were incubated in 96-well plates (5%  $\text{CO}_2$  at  $37^\circ\text{C}$ ) for 24 h. Then different concentrations (10, 20, 50,  $100 \mu\text{g}\cdot\text{mL}^{-1}$ ) of DAP-CDs solutions were added into each well, followed by incubation for 24 h. After that,  $50 \mu\text{L}$  MTT ( $1 \text{ mg}\cdot\text{mL}^{-1}$ ) was added into each well, incubated for another 4 h. The culture medium was then removed, and the obtained mixture was dissolved in  $100 \mu\text{L}$  DMSO and shaken for 10 min. The absorbance of each well was measured at 550 nm. The cell viability was estimated according to the equation:

$$\text{cell viability}(\%) = \text{OD}_s / \text{OD}_u$$

Where  $\text{OD}_s$  is obtained in the presence of DAP-CDs and  $\text{OD}_u$  is obtained in the absence of DAP-CDs.

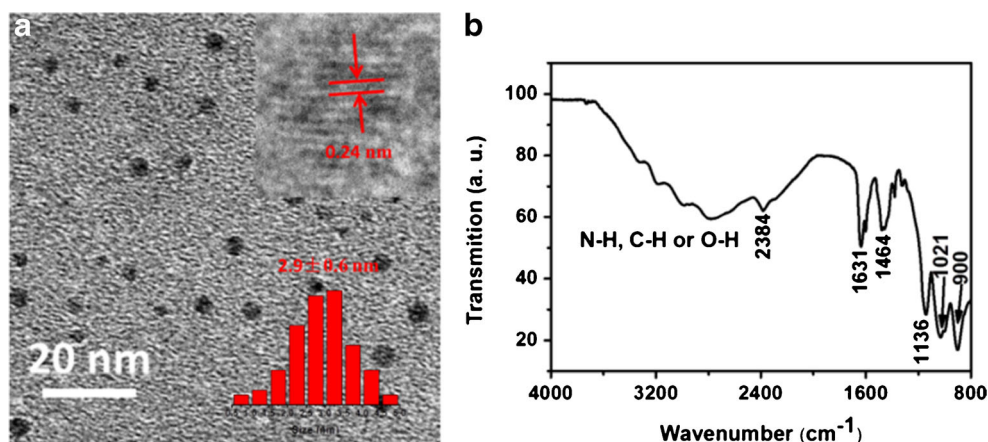
A549 and KB cells were treated with  $10 \mu\text{g}\cdot\text{mL}^{-1}$  DAP-CDs in culture media for 24 h at  $37^\circ\text{C}$ . Before imaging, the DAP-CDs loaded cells were rinsed three times, and incubated with 2 mL phosphate buffered solution (PBS) buffer (0.2 M) at  $\text{pH} = 7.0$  for 2 h. Images of the cells were immediately captured at ambient temperature on a confocal laser scanning microscopy.

## Results and discussion

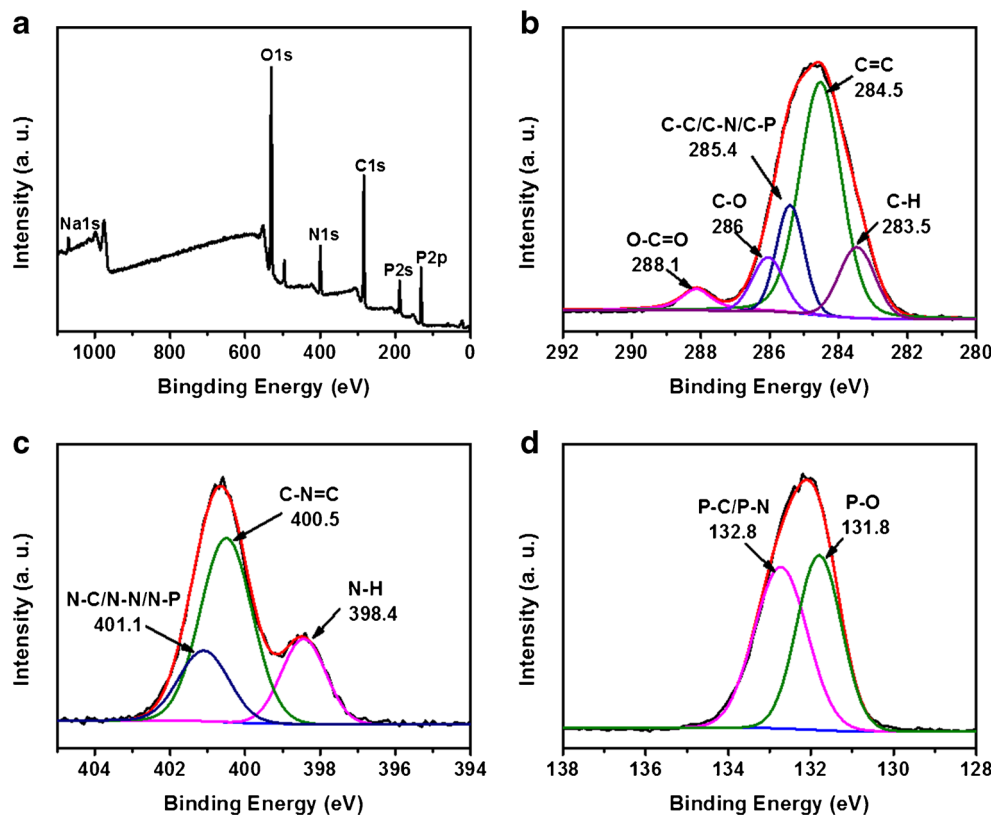
Figure 1a shows the HRTEM image and diameter distribution of DAP-CDs. It can be found that the as-prepared DAP-CDs are well dispersed spots with a lattice distance of ca. 0.24 nm, which is approximate to the (001) facet of graphite. The plots histogram of size distribution indicates that the sizes of DAP-CDs range from 0.5 to 5.0 nm with an average size of 2.9 nm. Figure 1b displays the Fourier-transform infrared (FT-IR) spectrum. The broad band ranging from  $2800 \text{ cm}^{-1}$  to  $3600 \text{ cm}^{-1}$  belongs to the characteristic vibration of N-H, C-H and O-H bonds. It is obviously found that the contents of N-H, and O-H are relatively lower than that of C-H. Due to cyano group is hard to form even at high temperature especially in aqueous solution, the peak at  $2384 \text{ cm}^{-1}$  can be attributed to the  $-\text{C} = \text{NH}^+$  group. The peak at  $1631 \text{ cm}^{-1}$  is corresponding to the characteristic vibration of  $\text{C} = \text{N}$  and  $1464 \text{ cm}^{-1}$  is relevant to  $\text{P} = \text{O}$  bond. The peaks  $1136$ ,  $1021$  and  $900 \text{ cm}^{-1}$  belong to stretching vibration of P-O, C-O, C-N or P-N bond.

Figure 2a shows the X-ray photoelectron spectra (XPS) survey spectrum, demonstrating that the as-prepared DAP-CDs are mainly composed of carbon, oxygen nitrogen, phosphorus and sodium with the binding energy peaks at 283.5, 397.9, 527.3, 190.8, 132.7 and 1070.9 eV, attributing to C 1 s, N 1 s, O 1 s, P 2 s, P 2p, and Na 1 s, respectively. The composition analysis of the DAP-CDs shows the elemental composition: carbon (45.5%), nitrogen (11.1%), oxygen (33.5%), phosphorus (9.6%), and sodium (0.3%), indicating

**Fig. 1** a HR-TEM image and diameter distribution, b FT-IR spectrum of DAP-CDs



**Fig. 2** XPS survey spectrum (a), C 1s (b), N 1s (c), and P 2p (d) XPS spectra of the as-prepared DAP-CDs



**Fig. 3** The formation process and structural model of DAP-CDs

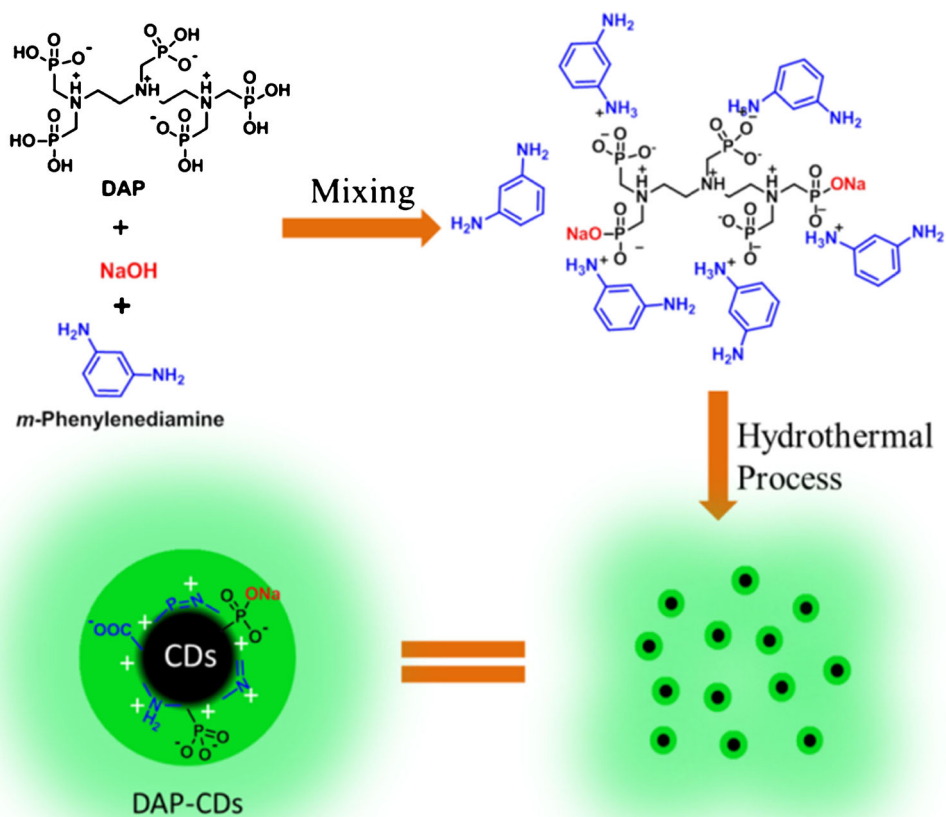


**Fig. 4** **a** Absorption and optimal emission spectra of DAP-CDs. **b** Excitation dependent emission spectra of DAP-CDs. Influence of **c** pH values, **d** ionic strengths, **e** metal cations, **(f)** Fe<sup>3+</sup> on the fluorescence intensity of DAP-CDs ( $\lambda_{\text{exc}} = 440 \text{ nm}$ )

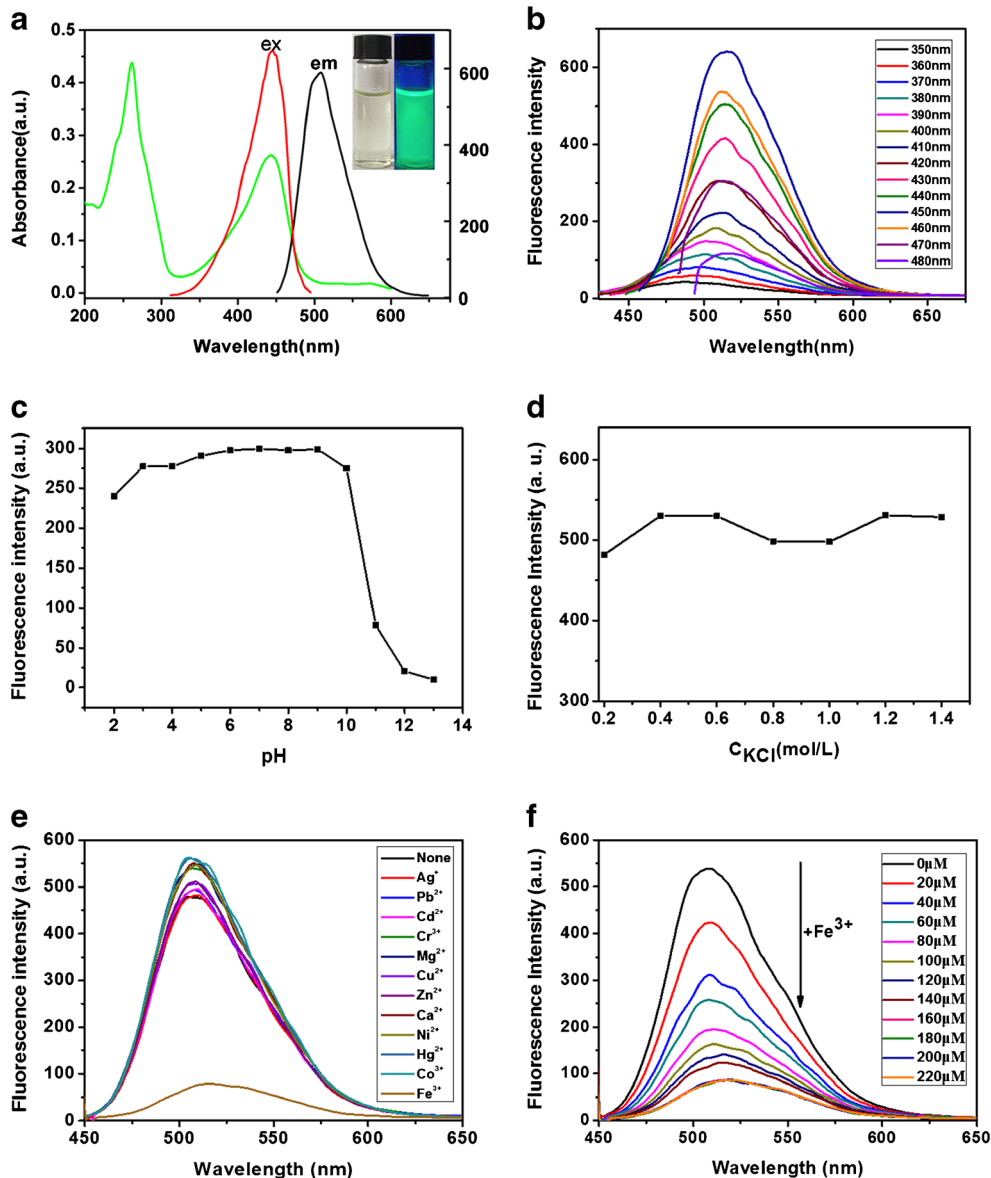
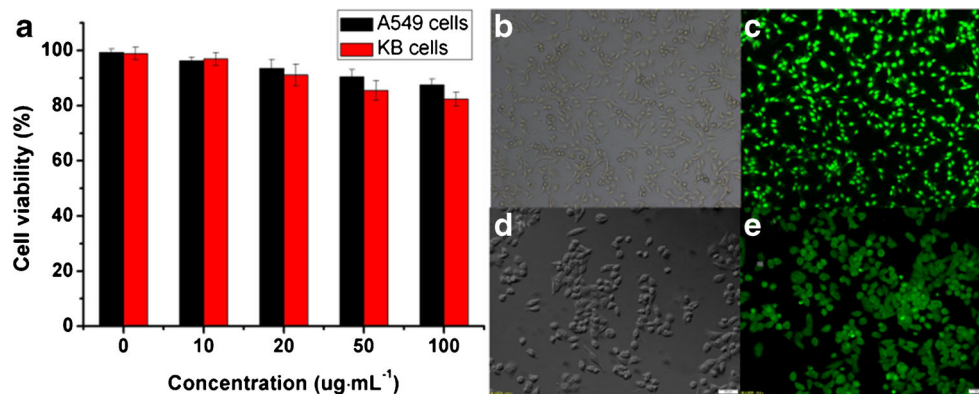


**Table 1** Comparison of present method with some other eco-friendly methods for preparing CDs

Carbon dots	Method	Emission color	Emission wavelengths (nm)	Quantum yield (%)	Ref.
S, N-CDs	Sulfuric Acid Carbonization	Blue	383	9	[26]
N-CDs	Hydrothermal Synthesis	Blue	454	23	[27]
N,P-CDs	Hydrothermal Synthesis	Blue to Green	430 to 500 (dual emissive)	30–78%	[28]
N,P-CDs	Microwave	Blue	418	17.5	[7]
RT-CDs	Magnetic Stirring	Blue	430	47	[29]
CDs	Hydrothermal Synthesis	Blue	440	13.3	[30]
CDs	Electrochemical Approach	Blue	439	10	[31]
DAP-CDs	Hydrothermal Synthesis	Green	510	32	This work

**Fig. 5** **a** Cellular cytotoxicity assessments of the DAP-CDs using the standard MTT assay toward A549 and KB cells. Confocal fluorescence image of the DAP-CDs under 465 nm laser excitation of KB (**b** and **c**) and A549 cells (**d** and **e**)



higher doping percentages of N and P elements than that of previously reported *N,P*-CDs.<sup>12</sup> The XRD pattern indicates that DAP-CDs is amorphous solid (Fig. S1). The zeta potential of DAP-CDs in deionized water is around 64 mV, indicating the surface of DAP-CDs is positive. Considering N element in the reagents DAP and aniline, we can infer the existence of  $-NH^+$  or  $-C=NH^+$  moiety on the surface of DAP-CDs. DAP-CDs can be well dispersed in water and keep stable at a concentration of 1 mg/mL for one year. Furthermore, the binding ability of DAP-CDs to moisture is very intensity, even under silica-gel drier. This phenomenon may be mainly originated from the positive surface. Due to a small amount of  $Na^+$  measured by XPS,  $PO_3^{2-}$  or  $COO^-$  should be connected to the surface of DAP-CDs.

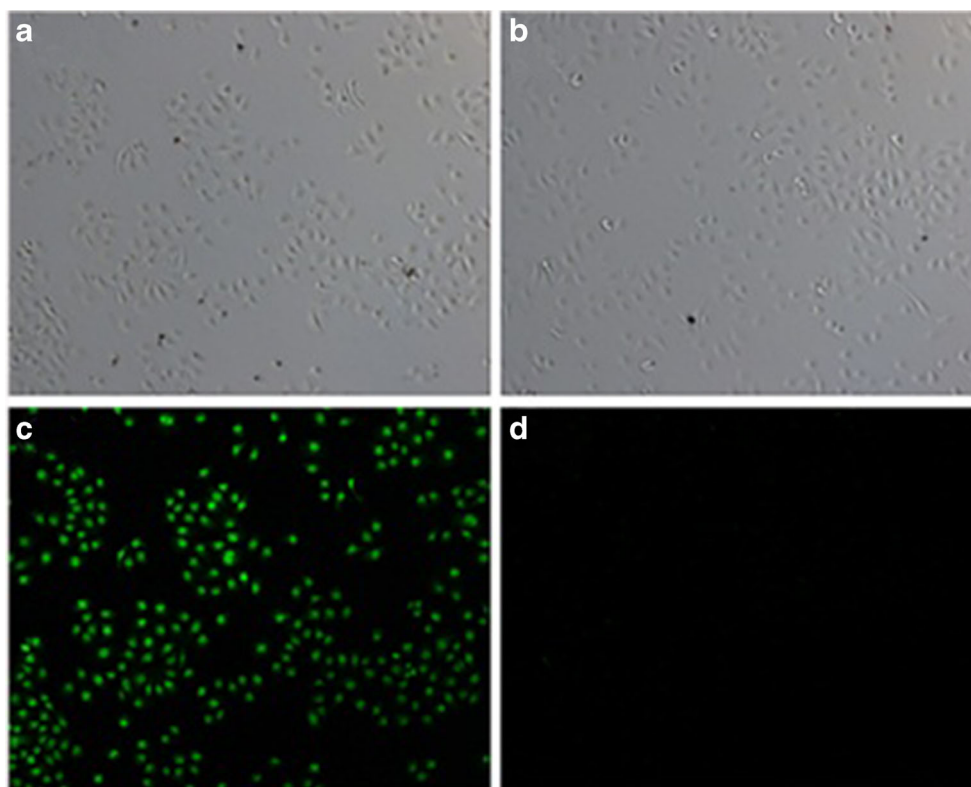
On the basis of the above analysis, the formation process of DAP-CDs is depicted in Fig. 3. Firstly, DAP functions with *m*-phenylenediamine through the acid-base reaction and then formed an organic ammonium salt. *m*-Phenylenediamine is insoluble in water, but its ammonium salt with DAP dissolves well. Then, some  $Na^+$  is introduced in the form of NaOH to form  $-PO_3Na_2$  or  $-PO_3HNa$ , which can enhance the hydrothermal stability of  $-PO_3^{2-}$  and retain some  $-PO_3^{2-}$  to control the size of final product. Under the hydrothermal condition, carbonizing process takes place and form nano-sized DAP-CDs.

The DAP-CDs in aqueous solution have two typical UV–vis absorption peaks at 262 and 443 nm, respectively. The peak at 262 nm, corresponding to the  $\pi-\pi^*$  transition of  $C=N$  or  $C=C$  bonds, leads to almost no observed fluorescent signal. The other transition centered at 443 nm due to the trapping of excited state energy by the surface states results in strong emission. The optimal excitation and emission wavelength are at 440 and 510 nm (Fig. 4a). Very bright green color under the excitation of UV (365 nm) light at a low concentration ( $5 \mu\text{g}\cdot\text{mL}^{-1}$ ) of the DAP-CDs aqueous solution can be clearly seen in the inset of Fig. 4a. Excitation-dependent fluorescent behavior is observed, which is common in fluorescent carbon nanomaterials. The emission wavelength shifts from 490 to 510 nm when the excitation wavelength increases from 350 to 480 nm (Fig. 4b). The QY of DAP-CDs is determined

to be 32%, which is higher than CDs prepared by some other ecofriendly methods [Table 1]. The fluorescence lifetime ( $\tau$ ) of DAP-CDs is assessed by fluorescent decay curves. As seen in Fig. S2, the fluorescent decay curve of DAP-CDs is recorded at 510 nm (excitation at 440 nm). We calculated the average lifetime of DAP-CDs to be 4.77 ns. The stability of both DAP-CDs under various conditions has also been studied. The fluorescent properties of DAP-CDs are pH dependent (Fig. 4c). The DAP-CDs displayed stable fluorescence in the pH range 2–10, indicating that the DAP-CDs can be employed in both acidic and basic environments. There are no changes in fluorescent intensity at high ionic strengths, which is significant because it is essential for DAP-CDs to be used in the presence of physical salt concentrations in practical applications (Fig. 4d). In addition, no obvious decrease of fluorescent intensity was measured when contacted with a broad range of metal cations including  $Ag^+$ ,  $Pb^{2+}$ ,  $Cd^{2+}$ ,  $Cr^{3+}$ ,  $Mg^{2+}$ ,  $Cu^{2+}$ ,  $Zn^{2+}$ ,  $Ca^{2+}$ ,  $Ni^{2+}$ ,  $Hg^{2+}$  and  $Co^{3+}$ , even at high concentrations (Fig. 4e). In spite of a serious quenching phenomenon can be observed at high concentration of  $Fe^{3+}$ , the DAP-CDs can be used for  $Fe^{3+}$  detection. Fig. 5f showed the fluorescence quenching of DAP-CDs at various concentrations of  $Fe^{3+}$  ions. With increasing  $Fe^{3+}$  ions concentration (up to  $220 \mu\text{M}$ ), the fluorescence intensity of DAP-CDs decreased progressively, revealing that the sensing system is sensitive to  $Fe^{3+}$  concentration. The linear range of  $Fe^{3+}$  detection is 0.09–60  $\mu\text{M}$  and the correlation coefficient ( $R^2$ ) is 0.986. The detection limit is estimated to be 0.09  $\mu\text{M}$  at a signal-to-noise ratio of 3. It is demonstrated that this DAP-CDs possesses distinctly enhanced resistance to ion interference, comparing to previous reported *N,P*-co-doping CDs which can be quenched by much lower concentration of  $Fe^{3+}$  ions [15].

In order to explore the biological applications, the cytotoxicity of DAP-CDs was evaluated using A549 and KB cells through MTT assays. As shown in Fig. 5a, the cell viability is above 85% after 24 h incubation of the A549 and KB cells with the DAP-CDs (10, 20, 50, 100  $\mu\text{g}\cdot\text{mL}^{-1}$ ). The cell viabilities are estimated to be higher than 87% and 82% upon addition of DAP-CDs with a high dose of 100  $\mu\text{g}\cdot\text{mL}^{-1}$  for

**Fig. 6** Confocal fluorescence images of A549 cells after incubation with DAP-CDs (**a, c**) DAP-CDs in pH 7.4 PBS buffer. (**b, d**) DAP-CDs + Fe<sup>3+</sup> in pH 7.4 PBS buffer. From top to bottom: bright field and fluorescent image excited with a 465 nm laser



24 h. As displayed in Fig. 5c, e, KB and A549 cells displays green fluorescence with blue excitation when incubated with the DAP-CDs ( $10 \mu\text{g}\cdot\text{mL}^{-1}$ ) only for 24 h at 37 °C. The confocal images show green emission in A549 and KB cells, indicating that the DAP-CDs can easily pass through cell membranes and enter into cells. Furthermore, the cell viability is very high evidenced by the confocal imaging, because of the low cellular cytotoxicity of DAP-CDs (Fig. 5). This sufficiently demonstrates that DAP-CDs have huge potential in the area of bio-imaging.

The A549 cells were seeded in the culture plate and cultured with  $10 \mu\text{g}\cdot\text{mL}^{-1}$  of DAP-CDs when the time increased from 30 min to 24 h. The photographs of the A549 cells were captured by a laser scanning confocal microscope. As obviously shown in Fig. S3, the A549 cells became quite bright, owing to the strong fluorescence from the DAP-CDs. As expected, the fluorescence brightness of A549 cells becomes quenching as introduction of exogenous Fe<sup>3+</sup> (200  $\mu\text{M}$ ) into the DAP-CDs treated A549 cells (Fig. 6). Therefore, the DAP-CDs are an effective probe for monitoring Fe<sup>3+</sup> in cells.

## Conclusions

In summary, we have synthesized a *N,P*-codoped DAP-CDs with highly doping ratios. This CDs emitted a strong green fluorescence under the excitation of 440 nm, and displayed water dispersibility, photo-stability in a broad range of pH

values as well as kept photo-stability when contacting with various metal ions. Huge potential in bio-imaging can be indicated by virtue of its high biocompatibility and high-quality cell imaging for A549 and KB cells. Furthermore, the DAP-CDs can also be used as an active probe for the monitoring Fe<sup>3+</sup> in both aqueous solution and living cells. Further investigations on designs and applications of highly *N,P*-doped CDs are in progress.

**Acknowledgements** Financial supports by the National Natural Science Foundation of China (NSFC) (grant number 51573078) are gratefully acknowledged.

**Compliance with ethical standards** The author(s) declare that they have no competing interests.

## References

1. Zuo P, Lu X, Sun Z, Guo Y, He H (2016) A review on syntheses, properties, characterization and bioanalytical applications of fluorescent carbon dots. *Microchim Acta* 183(2):519–542
2. Zhou J, Zhou H, Tang J, Deng S, Yan F, Li W, Qu M (2017) Carbon dots doped with heteroatoms for fluorescent bioimaging: a review. *Microchim Acta* 184(2):1–26
3. Pan L, Sun S, Zhang A, Jiang K, Zhang L, Dong C, Huang Q, Wu A, Lin H (2015) Truly fluorescent excitation-dependent carbon dots and their applications in multicolor cellular imaging and multidimensional sensing. *Adv Mater* 27(47):7782–7787

- Jiang K, Sun S, Zhang L, Wang Y, Cai C, Lin H (2015) Bright-yellow-emissive N-doped carbon dots: preparation, cellular imaging, and bi-functional sensing. *ACS Appl Mater Interfaces* 7(41):23231–23238
- Huang H, Lv JJ, Zhou DL, Bao N, Xu Y, Wang AJ, Feng JJ (2013) One-pot green synthesis of nitrogen-doped carbon nanoparticles as fluorescent probes for mercury ions. *RSC Adv* 3(44):21691–21696
- Jiang K, Sun S, Zhang L, Lu Y, Wu A, Cai C, Lin H (2015) Red, green, and blue luminescence by carbon dots: full-color emission tuning and multicolor cellular imaging. *Angew Chem Int Ed Engl* 54(18):5360–5363
- Li H, Shao FQ, Zou SY, Yang QJ, Huang H, Feng JJ, Wang AJ (2016) Microwave-assisted synthesis of N, P-doped carbon dots for fluorescent cell imaging. *Microchim Acta* 183(2):821–826
- Wang W, Lu YC, Huang H, Feng JJ, Chen JR, Wang AJ (2014) Facile synthesis of water-soluble and biocompatible fluorescent nitrogen-doped carbon dots for cell imaging. *Analyst* 139(7):1692–1696
- Huang H, Lu YC, Wang AJ, Liu JH, Chen JR, Feng JJ (2014) A facile, green, and solvent-free route to nitrogen–sulfur-codoped fluorescent carbon nanoparticles for cellular imaging. *RSC Adv* 4(23):11872–11875
- Lim SY, Shen W, Gao Z (2015) Carbon quantum dots and their applications. *Chem Soc Rev* 44(1):362–381
- Fernando KA, Sahu S, Liu Y, Lewis WK, Gulians EA, Jafariyan A, Wang P, Bunker CE, Sun YP (2015) Carbon quantum dots and applications in photocatalytic energy conversion. *ACS Appl Mater Interfaces* 7(16):8363–8376
- Ge J, Lan M, Liu W, Jia Q, Guo L, Zhou B, Meng X, Niu G, Wang P (2016) Graphene quantum dots as efficient, metal-free, visible - light-active photocatalysts. *Sci China Mater* 59(1):12–19
- Li H, He X, Kang Z, Huang H, Liu Y, Liu J, Lian S, Tsang CH, Yang X, Lee ST (2010) Water-soluble fluorescent carbon quantum dots and photocatalyst design. *Angew Chem Int Ed Engl* 49(26):4430–4434
- Wang X, Sun G, Li N, Chen P (2016) Quantum dots derived from two-dimensional materials and their applications for catalysis and energy. *Chem Soc Rev* 45(8):2239–2262
- Gong X, Zhang Q, Gao Y, Shuang S, Choi MM, Dong C (2016) Phosphorus and nitrogen dual-doped hollow carbon dot as a Nanocarrier for doxorubicin delivery and biological imaging. *ACS Appl Mater Interfaces* 8(18):11288–11297
- Shi B, Su Y, Zhang L, Huang M, Liu R, Zhao S (2016) Nitrogen and phosphorus co-doped carbon Nanodots as a novel fluorescent probe for highly sensitive detection of Fe(3+) in human serum and living cells. *ACS Appl Mater Interfaces* 8(17):10717–10725
- Sun X, Bruckner C, Lei Y (2015) One-pot and ultrafast synthesis of nitrogen and phosphorus co-doped carbon dots possessing bright dual wavelength fluorescence emission. *Nano* 7(41):17278–17282
- Li W, Zhang Z, Kong B, Feng S, Wang J, Wang L, Yang J, Zhang F, Wu P, Zhao D (2013) Simple and green synthesis of nitrogen-doped photoluminescent carbonaceous nanospheres for bioimaging. *Angew Chem Int Ed Engl* 52(31):8151–8155
- Wu ZL, Zhang P, Gao MX, Liu CF, Wang W, Leng F, Huang CZ (2013) One-pot hydrothermal synthesis of highly luminescent nitrogen-doped amphoteric carbon dots for bioimaging from *Bombyx mori* silk – natural proteins. *J Mater Chem B* 1(22):2868
- Wang L, Zhou HS (2014) Green synthesis of luminescent nitrogen-doped carbon dots from milk and its imaging application. *Anal Chem* 86(18):8902–8905
- Yang Z, Xu M, Liu Y, He F, Gao F, Su Y, Wei H, Zhang Y (2014) Nitrogen-doped, carbon-rich, highly photoluminescent carbon dots from ammonium citrate. *Nano* 6(3):1890–1895
- Bourlinos AB, Stassinopoulos A, Anglos D, Zboril R, Karakassides M, Giannelis EP (2008) Surface functionalized carbogenic quantum dots. *Small* 4(4):455–458
- Peng H, Travas-Sejdic J (2009) Simple aqueous solution route to luminescent Carbogenic dots from carbohydrates. *Chem Mater* 21(23):5563–5565
- Li H, He X, Liu Y, Huang H, Lian S, Lee S-T, Kang Z (2011) One-step ultrasonic synthesis of water-soluble carbon nanoparticles with excellent photoluminescent properties. *Carbon* 49(2):605–609
- Ding H, Yu SB, Wei JS, Xiong HM (2016) Full-color light-emitting carbon dots with a surface-state-controlled luminescence mechanism. *ACS Nano* 10(1):484–491
- Sun D, Ban R, Zhang P-H, Wu G-H, Zhang J-R, Zhu J-J (2013) Hair fiber as a precursor for synthesizing of sulfur- and nitrogen-codoped carbon dots with tunable luminescence properties. *Carbon* 64:424–434
- Wang L, Yin Y, Jain A, Zhou HS (2014) Aqueous phase synthesis of highly luminescent, nitrogen-doped carbon dots and their application as bioimaging agents. *Langmuir* 30:14270–14275
- Parvin N, Mandal TK (2017) Dually emissive P, N-co-doped carbon dots for fluorescent and photoacoustic tissue imaging in living mice. *Microchim Acta* 184(4):1117–1125
- Xia J, Zhuang YT, Yu YL, Wang JH (2017) Highly fluorescent carbon polymer dots prepared at room temperature, and their application as a fluorescent probe for determination and intracellular imaging of ferric ion. *Microchim Acta* 184(4):1109–1116
- Yan F, Kong D, Luo Y, Ye Q, He J, Guo X, Chen L (2016) Carbon dots serve as an effective probe for the quantitative determination and for intracellular imaging of mercury (II). *Microchim Acta* 183(5):1611–1618
- Li X, Zhao Z, Pan C (2016) Ionic liquid-assisted electrochemical exfoliation of carbon dots of different size for fluorescent imaging of bacteria by tuning the water fraction in electrolyte. *Microchim Acta* 183(9):2525–2532